

PAPR Reduction with Pre-chirp Selection for Affine Frequency Division Multiplexing

Haozhi Yuan, *Graduate Student Member, IEEE*, Yin Xu, *Member, IEEE*,

Xinghao Guo, *Graduate Student Member, IEEE*, Tianyao Ma, *Graduate Student Member, IEEE*,

Haoyang Li, *Graduate Student Member, IEEE*, Dazhi He, *Member, IEEE*, Wenjun Zhang, *Fellow, IEEE*

Abstract—Affine frequency division multiplexing (AFDM) is a promising new multicarrier technique based on discrete affine Fourier transform (DAFT). By properly tuning pre-chirp parameter and post-chirp parameter in the DAFT, the effective channel in the DAFT domain can completely avoid overlap of different paths, thus constitutes a full representation of delay-Doppler profile, which significantly improves the system performance in high mobility scenarios. However, AFDM has the crucial problem of high peak-to-average power ratio (PAPR) caused by phase randomness of modulated symbols. In this letter, an algorithm named grouped pre-chirp selection (GPS) is proposed to reduce the PAPR by changing the value of pre-chirp parameter on subcarriers group by group. Specifically, it is demonstrated first that the important properties of AFDM system are maintained when implementing GPS. Secondly, we elaborate the operation steps of GPS algorithm, illustrating its effect on PAPR reduction and its advantage in terms of computational complexity compared with the ungrouped approach. Finally, simulation results of PAPR reduction in the form of complementary cumulative distribution function (CCDF) show the effectiveness of the proposed GPS algorithm.

Index Terms—Affine frequency division multiplexing (AFDM), discrete affine Fourier transform (DAFT), peak-to-average power ratio (PAPR).

I. INTRODUCTION

The next generation wireless systems (beyond 5G/6G) is expected to suppose high mobility scenarios such as vehicle-to-everything (V2X) systems, high-speed railway systems, and aeronautical systems [1]. Since the high-speed relative motion between the transmitter and the receiver can cause excessive Doppler frequency shifts, the wireless channel exhibits fast time-varying properties. In 4G/5G standards, the widely utilized multicarrier technique, i.e., orthogonal frequency division multiplexing (OFDM), has poor robustness to carrier frequency offset (CFO) [2]. Therefore, the system performance deteriorates significantly in high-speed scenarios.

In this context, a series of next-generation waveforms are proposed. One of the promising representative multicarrier modulation techniques is affine frequency division multiplexing (AFDM) based on the discrete affine Fourier transform (DAFT) [3], [4]. By properly tuning two DAFT parameters, subchannels of different paths will be completely separate so that the representation of the effective channel in the DAFT domain becomes sparse and quasi-static. Therefore, AFDM can achieve the optimal diversity order in doubly dispersive channels. In addition, DAFT can be regarded as a generalization of discrete Fourier transform (DFT), which makes AFDM system fully compatible with OFDM system. Compared with

orthogonal time frequency space (OTFS), AFDM requires less pilot guard overhead and has lower modulation complexity [5].

Because of the enormous potential of AFDM for its excellent compatibility and significant advantages in high-speed communications, the current explorations of AFDM has become hot topics. Works for channel estimation and equalization are involved in [6] and [7], respectively. Index modulation (IM) is studied in [8] and [9] where the unique properties of AFDM is utilized.

AFDM faces the serious problem of high PAPR which is exactly the same as OFDM in theory. However, no studies on PAPR reduction currently exist. The high PAPR will cause saturation distortion of the power amplifier at the transmitter and ultimately deteriorate communication reliability. In OFDM, there are several ways for PAPR reduction, such as coding [10], Partial Transmission Sequence (PTS) [11], Tone Reservation (TR) [12], and some other schemes. In AFDM, the phases of the transmitted symbols in the DAFT domain are random. Through the inverse DAFT (IDAFT) module, the initial phases of subcarriers is determined by one of the alterable parameters. If the product of most symbols and the corresponding subcarriers within one block has the same or similar phases, then the signal in the time domain will have an extremely high peak.

In this letter, a grouped pre-chirp selection (GPS) algorithm is proposed to reduce the PAPR in AFDM. Here, the two alterable parameters in the DAFT/IDAFT module are termed as pre-chirp parameter and post-chirp parameter, respectively. Since the constraint of the pre-chirp parameter is loose, it is theoretically possible to achieve the minimum PAPR by going through all feasible values of the pre-chirp parameter on every subcarrier. In order to reduce the computational complexity, we group subcarriers to certain principles, and the unified value in each group is adjusted.

The remainder of this letter is organized as follows. Section II describes the system model with the proposed GPS based on conventional AFDM. Section III elaborates the specific operation of the GPS for PAPR reduction. Section IV shows and discusses the numerical results to verify the effectiveness of the proposed PAPR reduction algorithm. Section V concludes this letter.

II. SYSTEM MODEL

In this section, the conventional AFDM is briefly introduced firstly. Then, the AFDM model with GPS is described. The

difference between the two is highlighted. Furthermore, two important properties, i.e., orthogonality between subcarriers and non-overlapping of subchannels of AFDM, are proved to be unchanged through theoretical derivation.

A. Conventional AFDM

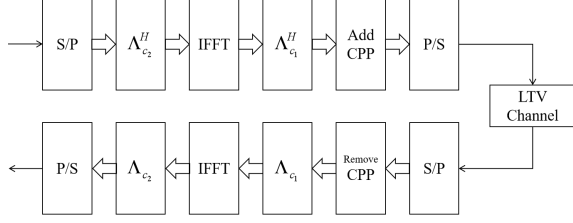


Fig. 1. AFDM block diagram.

The conventional AFDM block diagram is shown in Fig. 1. The data symbols are placed in the DAFT domain. At the transmitter, IDAFT is performed to map a sequence of data symbols from the DAFT domain into the time domain. At the receiver, DAFT is utilized to recover the data symbols. With N subcarriers, the IDAFT can be expressed as

$$s[n] = \frac{1}{\sqrt{N}} \sum_{m=0}^{N-1} x[m] \cdot e^{j2\pi(c_1 n^2 + c_2 m^2 + mn/N)}, \quad (1)$$

where $x[m]$ denotes the modulated symbol in the DAFT domain and $s[n]$ denotes the signal in the time domain. According to (1), the frequencies of all subcarriers vary periodically and linearly with time in AFDM.

The impulse response of the linear time-varying (LTV) channel can be expressed as

$$h_n[l] = \sum_{p=1}^P h_p e^{-j2\pi f_p n} \delta(l - l_p), \quad (2)$$

where P is the number of paths, $\delta(\cdot)$ is the Dirac delta function, and h_p , f_p , and l_p are the complex gain, Doppler shift, and the integer delay associated with the p -th path, respectively.

For transmitted data symbols in each block, the IDAFT, DAFT and the effect of doubly dispersive channel can all be expressed in matrix form.

The input-output relation in time domain, i.e., the effect of channel, can be formulated as

$$\mathbf{r} = \mathbf{H}\mathbf{s} + \mathbf{w}, \quad (3)$$

where $\mathbf{s}, \mathbf{r} \in \mathbb{C}^{N \times 1}$, $\mathbf{w} \sim \mathcal{CN}(\mathbf{0}, N_0 \mathbf{I}) \in \mathbb{C}^{N \times 1}$, and

$$\mathbf{H} = \sum_{p=1}^P h_p \mathbf{\Gamma}_{\text{CPP}_p} \mathbf{\Delta}_{f_p} \mathbf{\Pi}^{l_p}, \quad (4)$$

where $\mathbf{\Pi}$ is the permutation matrix

$$\mathbf{\Pi} = \begin{bmatrix} 0 & \cdots & 0 & 1 \\ 1 & \cdots & 0 & 0 \\ \vdots & \ddots & \ddots & \vdots \\ 0 & \cdots & 1 & 0 \end{bmatrix}_{N \times N}, \quad (5)$$

$\mathbf{\Delta}_{f_p}$ is the $N \times N$ diagonal matrix

$$\mathbf{\Delta}_{f_p} = \text{diag}(e^{-j2\pi f_p n}, n = 0, 1, \dots, N-1), \quad (6)$$

and $\mathbf{\Gamma}_{\text{CPP}_p}$ is a $N \times N$ diagonal matrix

$$\mathbf{\Gamma}_{\text{CPP}_p} = \text{diag}\left\{ \begin{array}{ll} e^{-j2\pi c_1(N^2 - 2N(l_p - n))} & n < l_p, \\ 1 & n \geq l_p, \end{array} \right. n = 0, \dots, N-1. \quad (7)$$

The DAFT matrix is expressed as

$$\mathbf{A} = \mathbf{\Lambda}_{c_2} \mathbf{F} \mathbf{\Lambda}_{c_1}, \quad (8)$$

where \mathbf{F} is the DFT matrix and

$$\mathbf{\Lambda}_c = \text{diag}(e^{-j2\pi c n^2}, n = 0, 1, \dots, N-1). \quad (9)$$

It is easy to find out that \mathbf{A} is a unitary matrix, thus the IDAFT matrix is

$$\mathbf{A}^{-1} = \mathbf{A}^H = \mathbf{\Lambda}_{c_1}^H \mathbf{F}^H \mathbf{\Lambda}_{c_2}^H. \quad (10)$$

Let $\mathbf{x} = [x[0], x[1], \dots, x[n]]^T \in \mathbb{C}^{N \times 1}$ denotes the symbols in the DAFT domain at the transmitter, where each of its elements is at the constellation point. Let $\mathbf{y} = [y[0], y[1], \dots, y[n]]^T \in \mathbb{C}^{N \times 1}$ denotes the received signals. Then the overall input-output relation in DAFT domain can be formulated as

$$\mathbf{y} = \mathbf{A}\mathbf{r} = \sum_{p=1}^P h_p \mathbf{A} \mathbf{\Gamma}_{\text{CPP}_p} \mathbf{\Delta}_{f_p} \mathbf{\Pi}^{l_p} \mathbf{A}^H \mathbf{x} + \mathbf{A}\mathbf{w} = \mathbf{H}_{\text{eff}} \mathbf{x} + \tilde{\mathbf{w}}, \quad (11)$$

where $\tilde{\mathbf{w}} \sim \mathcal{CN}(\mathbf{0}, N_0 \mathbf{I}) \in \mathbb{C}^{N \times 1}$ holds because \mathbf{A} is a unitary matrix.

According to [4], to achieve full diversity in LTV channels for integer Doppler shift, the pre-chirp parameter c_2 can be any irrational value while the minimum value of the post-chirp parameter c_1 is

$$c_1 = \frac{2\alpha_{\max} + 1}{2N}, \quad (12)$$

where α_{\max} is integer part of the maximum Doppler shift normalized with respect to the subcarrier spacing.

B. AFDM with GPS

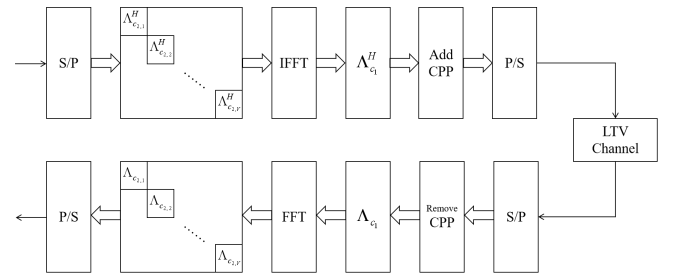


Fig. 2. AFDM with GPS block diagram.

The block diagram of AFDM with GPS is shown in Fig. 2. It can be seen that the pre-chirp module is the only module that differs from it in conventional AFDM. The modified module consists of different c_2 values in different groups of

subcarriers, where the time-domain signals can be expressed as

$$s[n] = \frac{1}{\sqrt{N}} \sum_{m=0}^{N-1} x[m] \cdot e^{j2\pi(c_1 n^2 + c_{2,m} m^2 + mn/N)}, \quad (13)$$

where $c_{2,m} \in \Omega_m$ represents the value of c_2 on m -th subcarrier, and Ω_m is the set of values of c_2 . This change is inspired by the loose constraint on c_2 value and for the purpose of lowering PAPR. It is worth considering whether the original properties of AFDM still hold, which will be detailed in the following.

First of all, it is evident that the sparse property of the effective channel \mathbf{H}_{eff} still exists. Since both $\mathbf{\Lambda}_{c_2}^H$ and $\mathbf{\Lambda}_{c_2}$ are diagonal matrices, simply changing the value of the diagonal elements do not effect on the positions of the non-zero elements.

In addition, the orthogonality between any two subcarriers remains the same based on the following derivation. Through IDAFT module, we consider two subcarriers having the same c_1 but different c_2 , which can be expressed as $e^{j2\pi(c_1 n^2 + c_{2,m_1} m_1^2 + m_1 n/N)}$ and $e^{j2\pi(c_1 n^2 + c_{2,m_2} m_2^2 + m_2 n/N)}$, respectively. c_{2,m_1} and c_{2,m_2} are any irrational numbers satisfying $c_{2,m_1} \neq c_{2,m_2}$. Then, we can derive their inner product as

$$\begin{aligned} & \sum_{n=0}^{N-1} e^{j2\pi(c_1 n^2 + c_{2,m_1} m_1^2 + m_1 n/N)} e^{-j2\pi(c_1 n^2 + c_{2,m_2} m_2^2 + m_2 n/N)} \\ &= e^{j2\pi(c_{2,m_1} m_1^2 - c_{2,m_2} m_2^2)} \sum_{n=0}^{N-1} e^{j\frac{2\pi}{N}(m_1 - m_2)n} \\ &= e^{j2\pi(c_{2,m_1} m_1^2 - c_{2,m_2} m_2^2)} \frac{1 - e^{j2\pi N(\frac{m_1 - m_2}{N})}}{1 - e^{j2\pi(\frac{m_1 - m_2}{N})}} \\ &= 0 \quad (0 \leq m_1 < m_2 \leq N-1). \end{aligned} \quad (14)$$

The derivation above demonstrates that such a change does not affect the orthogonality, which lays a foundation for our proposed GPS algorithm.

III. PROPOSED PAPR REDUCTION SCHEME

In this section, the proposed GPS algorithm for PAPR reduction is elaborated. Within each subblock, the expression of PAPR is written as

$$\text{PAPR} = \frac{P_{\max}}{P_{\text{avg}}} = \frac{\max_{n=0, \dots, N-1} (\|s[n]\|^2)}{\frac{1}{N} \sum_{n=0}^{N-1} \|s[n]\|^2}, \quad (15)$$

where $s[n]$ is the n -th sample of the time-domain signals. Note that PAPR is defined for continuous time bandpass signals. However, in the software simulation, the discrete time-domain signal $s[n]$ cannot reserve all peaks of the continuous time-domain signal $s(t)$, which will result in the PAPR measured value smaller than the actual value. Fortunately, with no less than 4-fold oversampling, $s[n]$ and $s(t)$ have the same PAPR [13]. To quantitatively represent the PAPR indicator, the complementary cumulative distribution function (CCDF) is adopted, which is given as

$$\text{CCDF} = \Pr(\text{PAPR} > \text{PAPR}_0), \quad (16)$$

where PAPR_0 denotes a certain level of PAPR value and $\Pr(\cdot)$ is the probability function.

Based on the fact that the properties of AFDM remain unchanged after altering the value of c_2 on each subcarrier, there is room for PAPR reduction. Specifically, finite sets Ω_m ($m = 0, \dots, N-1$) whose elements are all irrational are created initially. It is assumed that the number of elements in every set Ω_m is W . Then, by traversing all possible values on every subcarrier, the optimal PAPR value can finally be reached. However, the computing cost of this method is extremely high since the result of each PAPR calculation corresponds to one IFFT matrix multiplication and one post-chirp matrix multiplication. Totally, W^{N-1} times calculations are required in order to get the final result. Note that the first subcarrier where $m = 0$ does not need any change because the initial phase is constant 0 according to (13).

Given that the computational complexity of the method above is too high, the following three aspects need to be taken into account in order to achieve a better balance between performance and computing complexity.

At first, the principle for selecting values of elements in Ω_m is considered. According to (13), the phase of each term in the summation process can be expressed as $\angle(x[m]) + 2\pi(c_1 n^2 + c_{2,m} m^2 + mn/N)$, where $x[m]$ generates the phase randomness. Note that when the subcarriers number N is large, the phase randomness does not affect the average power, but rather causes large fluctuations in the peak power. Therefore, reducing the peak power should be focused on. For simplicity, the case where the set has two elements is firstly considered. Going through the pre-chirp module is equivalent to rotating the phase of each data symbol. Since the algorithm screens for the smallest PAPR result, the phase difference of the two elements should be made as large as possible. This is because the expectation of the peak power is constant regardless of the rotation so that a larger variance implies a smaller minimum peak power in a probabilistic sense. Guided by this principle, the optimal value of phase difference should be π . In the form of formula, it can be written as

$$2\pi c_{2,m} m^2 = \pm \frac{\pi}{2}. \quad (17)$$

Then, the value of pre-chirp on each subcarrier is given as

$$c_{2,m} = (-1)^i \frac{1}{4m^2}, \quad (18)$$

where $i = 0, 1$, corresponding to the two elements in Ω_m . However, the pre-chirp value should be irrational, so equation (18) is replaced with

$$c_{2,m} = (-1)^i \frac{\pi \cdot 10^k}{4m^2 \lfloor \pi \cdot 10^k \rfloor}, \quad (19)$$

where $\lfloor \cdot \rfloor$ represents the downward rounding operation and k determines how many decimals are retained. This principle can be generalized to the case where Ω_m contains W ($W \geq 2$) elements. The W feasible values of the pre-chirp parameter on the m -th subcarrier are

$$c_{2,m} = \frac{i\pi \cdot 10^k}{Wm^2 \lfloor \pi \cdot 10^k \rfloor}, \quad (20)$$

where $i = 0, \dots, W - 1$. The increase in the number of elements in Ω_m evidently favors PAPR reduction. However, as W increases, the phase difference between the elements inevitably decreases. As the result, the performance improvement becomes progressively slower while the complexity is linearly increasing. Therefore, with the aim of a good balance of performance and complexity, simply placing two elements in each Ω_m may be reasonable.

Moreover, using a non-traversal algorithm with fewer iterations can significantly reduce the complexity. Specifically, we sequentially select the pre-chirp values in Ω_m on all subcarriers, rather than traversing all permutation possibilities. At each pre-chirp change, if such a change reduces the PAPR, the change is permanently retained, otherwise it is restored. The computational complexity is reduced to a large extent using this algorithm. To be precise, with 2 possible values to take on each subcarrier, the original traversal algorithm requires 2^{N-1} iterations, while the suboptimal algorithm takes only $N - 1$ iterations. On the other hand, the performance loss is acceptable, as will be shown in simulations.

The complexity will be further reduced by grouping the subcarriers. The number of subcarriers included in any one group is arbitrary in principal, but it seems appropriate to set each group with equal size. Let V and M denote the number of groups and the number of subcarriers per group, respectively, where $N = V \cdot M$. For each data block, the number of iterations is further reduced from $N - 1$ to V by grouping. What's more, we find that the adjacent grouping approach performs better in reducing PAPR compared to the comb grouping approach, even though the complexity of both is the same. However, the optimal grouping approach still needs to be explored.

The proposed GPS algorithm for PAPR reduction is summarized in Algorithm 1. We initialize the pre-chirp value on every subcarrier to be positive number with $k = 2$, i.e., $c_{2,m} = \frac{\pi}{12.56m^2}$, $m = 0, \dots, N - 1$. Thus, the initialized pre-chirp matrix can be written as

$$\Lambda_{c_2}^{(0)} = \begin{bmatrix} 1 & 0 & \cdots & 0 \\ 0 & e^{j\frac{2\pi^2}{12.56}} & \cdots & 0 \\ \vdots & \vdots & \ddots & \vdots \\ 0 & 0 & \cdots & e^{j\frac{2\pi^2}{12.56}} \end{bmatrix}_{N \times N}. \quad (21)$$

The corresponding initialized PAPR is then calculated by

$$\text{PAPR}^{(0)} = \frac{\max(|\Lambda_{c_1}^H \mathbf{F}^H \Lambda_{c_2}^{H(0)} \mathbf{x}|^2)}{\text{mean}(|\Lambda_{c_1}^H \mathbf{F}^H \Lambda_{c_2}^{H(0)} \mathbf{x}|^2)}. \quad (22)$$

At each iteration, the pre-chirp values in one group are all reversed. Then, a new $\text{PAPR}^{(1)}$ is calculated by a new pre-chirp matrix $\Lambda_{c_2}^{(1)}$. At the end of the algorithm, the minimum PAPR of $(V+1)$ values and the corresponding pre-chirp matrix are selected as output, which are denoted as PAPR_{\min} and $\Lambda_{c_2, \min}$, respectively.

IV. NUMERICAL RESULTS

In this section, we provide numerical results to verify the effectiveness of the proposed GPS algorithm for PAPR reduction.

Algorithm 1: GPS algorithm in AFDM System for PAPR Reduction

Input: Number of subcarriers N , number of groups V , number of elements per group M , post-chirp matrix Λ_{c_1} , FFT matrix \mathbf{F} , symbol vector \mathbf{x} ;

- 1: Initialize $\Lambda_{c_2}^{(0)}$ and $\text{PAPR}^{(0)}$ as (21) and (22), respectively;
- 2: $\text{PAPR}_{\min} = \text{PAPR}^{(0)}$;
- 3: **for** $i = 1 : V$ **do**
- 4: $\Lambda_{c_2}^{(i)} = \Lambda_{c_2}^{(i-1)}$;
- 5: $\Lambda_{c_2}^{(i)}((i-1)M+1:iM) = \Lambda_{c_2}^{(i)}((i-1)M+1:iM)^H$;
- 6: Calculate $\text{PAPR}^{(i)}$ according to (23);
- 7: **if** $\text{PAPR}^{(i)} \geq \text{PAPR}_{\min}$ **then**
- 8: $\Lambda_{c_2}^{(i)}((i-1)M+1:iM) = \Lambda_{c_2}^{(i)}((i-1)M+1:iM)^H$;
- 9: **else**
- 10: $\text{PAPR}_{\min} = \text{PAPR}^{(i)}$;
- 11: **end if**
- 12: **end for**
- 13: $\Lambda_{c_2, \min} = \Lambda_{c_2}^{(V)}$;

Output: PAPR_{\min} and $\Lambda_{c_2, \min}$.

We consider an AFDM system with 16QAM under LTV channel. Without loss of generality, we have $h_i \sim \mathcal{CN}(0, 1)$. In addition, we set $N = 64$, $W = 2, 3, 4$, $V = 4, 8, 16$, and $k = 2$, respectively.

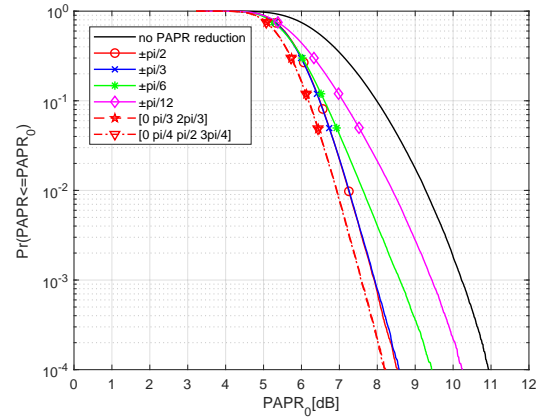


Fig. 3. PAPR performance of 16QAM/AFDM system with GPS for different number and values of elements in Ω_m .

In Fig. 3, simulation results of GPS with different values and numbers of elements in Ω_m are provided, where $V = 4$ and the grouping approach is adjacent grouping. In terms of values of elements, the result illustrates that larger phase difference will bring better performance for PAPR reduction. In terms of number of elements, the performance gain from the increase in number is very limited and converges quickly. For instance, when targeting the CCDF at a level of 10^{-4} , the performance of $W = 4$ is almost the same as $W = 3$.

Fig. 4 shows the difference in PAPR reduction performance for different number of groups and different grouping strategies. It can be observed that adjacent grouping is always better than comb grouping. Targeting the CCDF at a level of 10^{-4} , the adjacent grouping approach has approximately

0.7 dB, 0.3 dB, and 0.1 dB performance gain compared to the comb grouping approach with 4, 8, 16 groups, respectively. On the other hand, as the number of groups increases, the performance of PAPR reduction improves. However, the performance growth gradually slows down. Considering the complexity and performance tradeoffs, the number of groups should be kept as small as possible provided that the amplifier condition at the transmitter is met.

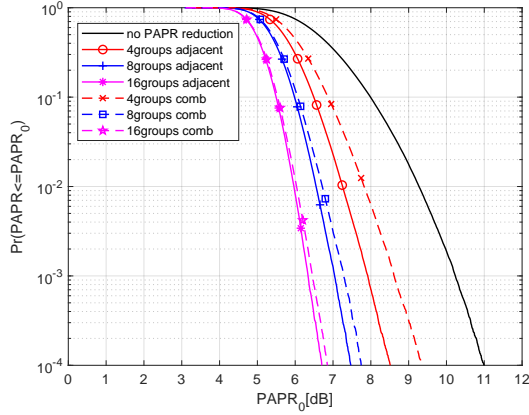


Fig. 4. PAPR performance of 16QAM/AFDM system with GPS algorithm for different number of subcarriers per group and grouping approach.

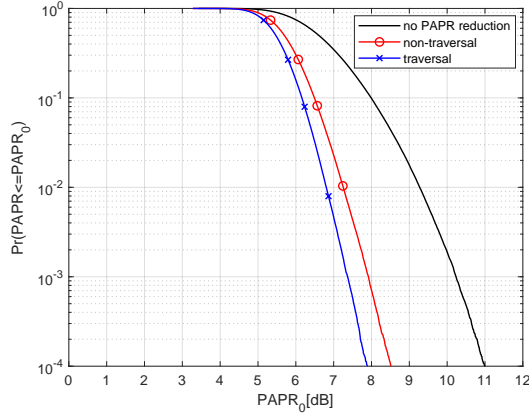


Fig. 5. PAPR performance of 16QAM/AFDM system with GPS for traversal algorithm and non-traversal algorithm.

Fig. 5 shows the performance difference between the traversal algorithm and the non-traversal algorithm. When the CCDF reaches 10^{-4} , the traversal algorithm has a performance gain of about 0.5 dB over the non-traversal algorithm, while the computational complexity is 4 times higher in the case of 4 groups. Since the performance gain is limited and the additional complexity is too high, we consider the non-traversal algorithm to be more practicable.

V. CONCLUSION

In this letter, a GPS algorithm is proposed to reduce PAPR in AFDM. We first make an adjustment to the pre-chirp module of the conventional AFDM and demonstrate that such an adjustment do not affect the nature of AFDM. Then, we discuss

several factors in GPS in order to achieve the best balance between performance and complexity. The performance of the proposed GPS algorithm is shown in simulations, which proves the effectiveness of it. However, only adjacent grouping approach and comb grouping approach are considered, and the number of subcarriers in each group is set equal. These may not be the optimal schemes for PAPR reduction, which can be an interesting research direction in the future.

REFERENCES

- [1] G. Liu, Y. Huang, N. Li, J. Dong, J. Jin, Q. Wang, and N. Li, "Vision, requirements and network architecture of 6g mobile network beyond 2030," *China Communications*, vol. 17, no. 9, pp. 92–104, 2020.
- [2] Y. Xu, J. Jiang, D. He, and W. Zhang, "A nb-iot random access scheme based on change point detection in ntms," *IEEE Open Journal of the Communications Society*, vol. 4, pp. 2176–2185, 2023.
- [3] A. Bemani, N. Ksairi, and M. Kountouris, "Afdm: A full diversity next generation waveform for high mobility communications," in *2021 IEEE International Conference on Communications Workshops (ICC Workshops)*, 2021, pp. 1–6.
- [4] —, "Affine frequency division multiplexing for next generation wireless communications," *IEEE Transactions on Wireless Communications*, vol. 22, no. 11, pp. 8214–8229, 2023.
- [5] H. S. Rou, G. T. F. de Abreu, J. Choi, M. Kountouris, Y. L. Guan, O. Gonsa *et al.*, "From ofdm to afdm: A comparative study of next-generation waveforms for isac in doubly-dispersive channels," *arXiv preprint arXiv:2401.07700*, 2024.
- [6] H. Yin and Y. Tang, "Pilot aided channel estimation for afdm in doubly dispersive channels," in *2022 IEEE/CIC International Conference on Communications in China (ICCC)*, 2022, pp. 308–313.
- [7] A. Bemani, N. Ksairi, and M. Kountouris, "Low complexity equalization for afdm in doubly dispersive channels," in *ICASSP 2022 - 2022 IEEE International Conference on Acoustics, Speech and Signal Processing (ICASSP)*, 2022, pp. 5273–5277.
- [8] Y. Tao, M. Wen, and Y. Ge, "Affine frequency division multiplexing with index modulation," *arXiv preprint arXiv:2310.05475*, 2023.
- [9] G. Liu, T. Mao, R. Liu, and Z. Xiao, "Pre-chirp-domain index modulation for affine frequency division multiplexing," *arXiv preprint arXiv:2402.15185*, 2024.
- [10] R. Roshan, J. Jain, and A. Soni, "Reduction of peak to average power ratio in ofdm technique by using cyclic codes," in *2013 International Conference on Intelligent Systems and Signal Processing (ISSP)*, 2013, pp. 233–237.
- [11] M.-J. Li and H.-Y. Liang, "Papr reduction of ofdm signals using partial transmit sequences with modified phase generation mechanism," in *2021 International Conference on Technologies and Applications of Artificial Intelligence (TAAI)*, 2021, pp. 266–269.
- [12] H. Li, N. Yang, Y. Xu, X. Ou, D. He, and Y. Guan, "On the papr of the lte-based 5g terrestrial broadcast system," in *2023 IEEE International Symposium on Broadband Multimedia Systems and Broadcasting (BMSB)*, 2023, pp. 1–6.
- [13] T. Jiang and Y. Wu, "An overview: Peak-to-average power ratio reduction techniques for ofdm signals," *IEEE Transactions on Broadcasting*, vol. 54, no. 2, pp. 257–268, 2008.